



Preparation and characterization of TiO₂-masked Fe₃O₄ nano particles for enhancing catalytic combustion of 1,2-dichlorobenzene and incineration of polymer wastes

Jin Seong Choi^a, Hyun Ki Youn^a, Bu Ho Kwak^a, Qiang Wang^b, Kyung Shik Yang^c, Jong Shik Chung^{a,b,*}

^a Department of Chemical Engineering, POSTECH (Pohang University of Science and Technology), San31, Hyoja-Dong, Nam-Gu, Pohang 790-784, Republic of Korea

^b School of Environmental Science and Engineering, POSTECH (Pohang University of Science and Technology), San31, Hyoja-Dong, Nam-Gu, Pohang 790-784, Republic of Korea

^c Chemistry and Biotechnology Examinations Bureau, Korean Intellectual Property Office, Government Complex-Daejeon, 139 Seonsa-ro, Seo-gu, Daejeon, Republic of Korea

ARTICLE INFO

Article history:

Received 17 February 2009

Received in revised form 7 May 2009

Accepted 22 May 2009

Available online 27 May 2009

Keywords:

TiO₂-masked iron oxides

Isoelectric point

1,2-dichlorobenzene oxidation

Catalyst-embedded polymer

Polymer incineration

ABSTRACT

Nano-sized Fe₃O₄ particles that were covered with a porous layer of nano-sized TiO₂ (TiO₂-masked Fe₃O₄) were prepared by simply controlling pH of aqueous slurry solution containing the two particles that have different values of isoelectric point (IEP coating method). The prepared sample showed an effective masking of red-brown color of Fe₃O₄ particles into a pale yellow. XPS and TEM measurements confirmed an effective covering of TiO₂ particles to the Fe₃O₄ surface. XANES analyses revealed the transformation of some Fe²⁺ ions into Fe³⁺ in the Fe₃O₄ structure (formation of Fe₃O_{4+δ}) due to a close interaction between Fe₃O₄ and TiO₂ during the IEP coating, which was not observed in physical mixture of dry powders of Fe₃O₄ and TiO₂. Compared with pure Fe₃O₄ or the physical mixture, TiO₂-masked Fe₃O₄ particles exhibited an activity enhancement for both catalytic oxidation of 1,2-dichloro benzene and thermal incineration of catalyst-embedded polyethylene and polystyrene. Temperature-programmed reduction of CO and temperature-programmed surface reaction of CO with O₂ revealed that oxygen vacancy sites on Fe₃O_{4+δ} played roles for the adsorption and reaction of CO, and close TiO₂ provided oxygen to the Fe₃O_{4+δ} sites. Compared with pure Fe₃O₄ particles, TiO₂-masked Fe₃O₄ particles also provided a good color-masking effect when embedded in polymers and improved the thermal stability of base polymers for high temperature fabrication.

© 2009 Elsevier B.V. All rights reserved.

1. Introduction

Nowadays, more polymeric wastes have been conveniently incinerated rather than being landfilled. The emission gas from an incinerator, however, contains various pollutants such as SO_x, NO_x, particulate matter, and chlorinated volatile organic compounds (VOCs). Polychlorinated dibenzodioxins (PCDDs) and dibenzofurans (PCDFs), so called dioxins, are also generated during the incineration [1,2]. Many countries in the world regulate emission levels of these materials from incinerators due to their toxicities [3–5].

Many research groups have focused on catalytic decomposition of dioxins or noxious pollutants at the end-of-pipe converters of the incineration systems. Noble metals such as Pt, Pd and Ir, which are very expensive, were reported to be active for dioxin decomposition [6,7]. Several transition metal oxides, such as

chromium oxides [8] and V₂O₅–WO₃ [9], have been investigated as potential catalysts as well.

Recently, attempts of embedding catalysts inside polymer have been made to reduce the pollutant emission during the incineration of polymeric wastes [10–13]. In this concept, catalysts were pre-mixed in polymer materials before or during the fabrication stage such as extrusion, casting, blow molding of pipe, bottle, film, etc. Catalysts in the polymers were used to prevent the formation of noxious pollutants or dioxins during the incineration of polymeric wastes. Several particles of silica [10], alumina [10], zeolite [10,11] and activated carbon [12] were tested, but studies are focused mainly on the formation of hydrocarbon intermediates during thermal cracking of polymeric materials in air. Iron-based catalysts would be a good candidate owing to their environmental safety. Imai et al. [13] reported that nano-sized particles of α-FeOOH dispersed in polyethylene were active to some extent for reducing dioxins, but its brown color limited its usage.

For practical purpose of embedding catalysts inside polymer, one has to consider several criteria when the catalyst/polymer composites are fabricated into various products: (1) catalyst

* Corresponding author. Tel.: +82 54 279 2267; fax: +82 54 279 8453.
E-mail address: jsc@postech.ac.kr (J.S. Chung).

particles should be small (nanoscale) for dispersion inside polymer products; (2) should be colorless; and (3) do not degrade the base polymer during the fabrication stage. Of course, catalysts should possess a high oxidative activity for complete combustion of polymeric wastes into CO₂ without forming noxious pollutants or dioxins.

In this work, we present preparation of TiO₂-coated Fe₃O₄ catalyst by simply adjusting pH of an aqueous slurry solution containing nano-sized particles of Fe₃O₄ and TiO₂ that have different values of isoelectrostatic point. Prepared catalyst samples were investigated for the oxidative characteristics in the catalytic oxidation of 1,2-dichlorobenzene and thermal incineration of catalyst-embedded polymers. Based on characterization of catalysts and catalyst-embedded polymers, active sites and reaction mechanism were suggested to explain the enhanced catalytic activity.

2. Experimental

2.1. Preparation of TiO₂-masked Fe₃O₄ catalysts

Nano-sized Fe₃O₄ (magnetite, FeO·Fe₂O₃) particles were prepared as reported by Kang et al. [14]. 10.3 mL of 1N HCl and 25 mL of purified, deoxygenated water were mixed. 8.65 g of FeCl₃·6H₂O and 3.18 g of FeCl₂·4H₂O (ratio of Fe(II)/Fe(III) = 1/2) were dissolved in the solution with vigorous stirring. The mother solution was dropped into 250 mL of 1.5 M NaOH solution under vigorous stirring. Precipitate was centrifuged at 4000 rpm and washed with purified deoxygenated water repeatedly until no separate precipitate was found at the bottom of water solution. Finally, the water solution having dispersed nano-sized iron oxide particles were filtered with an ultra filtration membrane (Millipore, pore size 25 nm) and dried at room temperature.

Particles in aqueous solution have their own isoelectric point (IEP) at which the surface charge becomes neutral at a certain pH. Two particles having different IEP values could have opposite surface charges at a certain pH so that attraction will occur between two particles. We utilize this principle to coat Fe₃O₄ particle with TiO₂ particles. 0.1 g nano-sized particles of prepared Fe₃O₄ or TiO₂ (HOMBIKAT, UV100) were dispersed in 200 ml water solution of pH 6 under ultra sonification for 2 min. At this pH, the surface charge of Fe₃O₄ in the solution is expected to be positive, and that of TiO₂ be negative. The two solutions were mixed at 1/19 volumetric ratio (1/19 weight ratio of Fe₃O₄/TiO₂) and subjected to sonification for 2 min so that Fe₃O₄ particle was coated with TiO₂ particles. The solution was then filtered using ultra filtration membrane and dried at room temperature. We also prepared physically mixed TiO₂ and Fe₃O₄ by mixing the two solid TiO₂ and Fe₃O₄ samples with 1/19 weight ratio of Fe₃O₄/TiO₂ for 1 h using a rotating machine.

2.2. Preparation of catalyst-embedded polymers

5–10 wt.% of catalyst particles were uniformly dispersed into PE polymer using an electrically heated mixer (Brabender). The mixer was heated to 200 °C. The screw speed was set to 50 RPM. PE chips (density: 0.962 g/cm³ at 25 °C) and catalysts were added sequentially, and let them blended for 7 min before being removed from the mixer. Catalyst-embedded PS (density: 1.04 g/cm³ at 25 °C) compounds were also prepared by the same procedure.

2.3. Characterization of catalysts and catalyst-embedded polymers

The phases of catalyst particles were confirmed by using XRD (MAC Science Co., M18XHF). The surface charges of Fe₃O₄ and TiO₂ were measured by using a potentiostat (EG&G PRINCETON

APPLIED RESEARCH, 263A). The surface status of catalysts was analyzed by using X-ray photoelectron spectroscopy (XPS, VG SCIENTIFIC, ESCALAB 220 i XL) with Mg K α radiation (1253.6 eV). X-ray absorption spectra (XAS) of the Fe K-edge were recorded at the Pohang Accelerator Laboratory (PAL) on a beam line BL3C1 operating at 2.5 GeV with ca. 100–160 mA. The radiation was monochromatized using a Si(1 1 1) double crystal monochromator and the incident beam was detuned by 25% using a piezoelectric translator in order to minimize contamination from higher harmonics, in particular, the third-order reflection of the silicon crystals. The energy resolution was 2×10^{-4} . Data were collected at room temperature in transmission mode. The intensities of incident and transmitted beams were measured by ionization detectors containing N₂. We calibrated the absorption energy by measuring the X-ray absorption spectrum of Fe metal foil and assigning the first inflection point in the absorbance–energy curve to 7112 eV. The XANES analysis was processed with Athena software (Version 0.8.041).

Temperature-programmed reduction of CO gas (CO-TPR) and temperature-programmed surface reaction (TPSR) of CO with O₂ were carried out in a packed-bed reactor made of 1/4" quartz tubing that was connected to mass spectrometer (HP, model 5973). The heating rate of the reactor was kept at 5 °C/min during the temperature-programmed analyses. For the CO-TPR, a reducing gas of 1% CO in He balance was passed through the reactor having 0.1 g of catalyst at a flow rate of 30 cm³/min. For the TPSR between CO and O₂, a mixture stream of 1% CO in He balance and 3.5% O₂ in He balance was passed through the reactor having 0.1 g catalyst at a flow rate of 15 cm³/min.

Thermal stabilities of polymer composites were characterized by means of thermogravimetric analysis (TGA, PerkinElmer, TGS-2). The samples were heated in air from 100 to 700 °C at a rate of 10 °C/min.

2.4. Catalytic activity tests

Activities of the prepared catalysts were evaluated in a packed-bed reactor made of 1/4" quartz tube for 1,2-dichlorobenzene (*o*-DCB) oxidation, which is commonly used as a model compound of dioxin due to its similar oxidation behavior [15]. Inlet concentration of DCB in the feed was controlled at 1000 ppm by passing air through a bubbling saturator whose temperature was controlled at 16.7 °C by using a circulator bath (JSRC-13C, JS Research Inc.). Weight hourly space velocity (WHSV) was kept at 6 L/h/g-cat.

2.5. Incineration tests of polymer samples

Emission gases during the incineration of various polymer chips were analyzed. The samples (0.1 g of each) were incinerated in the packed-bed reactor. The temperature was ramped at rate of 5 °C/min from 200 to 800 °C with an air flow of 50 cm³/min. CO₂ emitted during incineration of the polymer was detected at the reactor outlet with CO₂ analyzer (Thermo Scientific, 42C).

3. Results and discussion

3.1. TiO₂-masked Fe₃O₄ catalysts

The color of prepared particles of pure iron oxide was reddish-brown in air and water, as shown in Fig. 1. Most of particles were spherical in shape and uniform in size around 30 nm, and some particles changed to needle shape. XRD patterns shown in Fig. 2 match with peaks of Fe₃O₄ [16,17], having both cubic and orthorhombic structures. The average size of the particles was found to be about 30 nm when calculated by using the Scherrer equation [18].

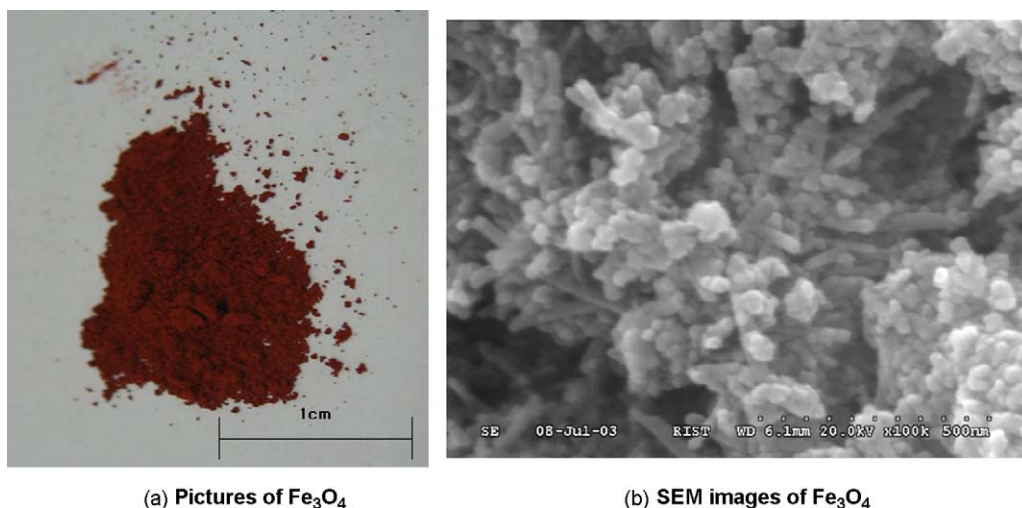


Fig. 1. Images of synthesized Fe_3O_4 . (a) Picture of Fe_3O_4 particles and (b) SEM image of Fe_3O_4 .

Surface charges (Zeta potential) of Fe_3O_4 and TiO_2 particles were measured in the pH range of 2–12 as shown in Fig. 3. The zeta potential of Fe_3O_4 changes from (+) to (–) at pH 8.5 and that of TiO_2 changes from (+) to (–) at about pH 5. It is therefore expected that, at pH range above 5 and below 8, Fe_3O_4 possesses positive surface charge whereas TiO_2 has negative charge so that an attractive force would adhere two particles together. Thus, we let the catalyst

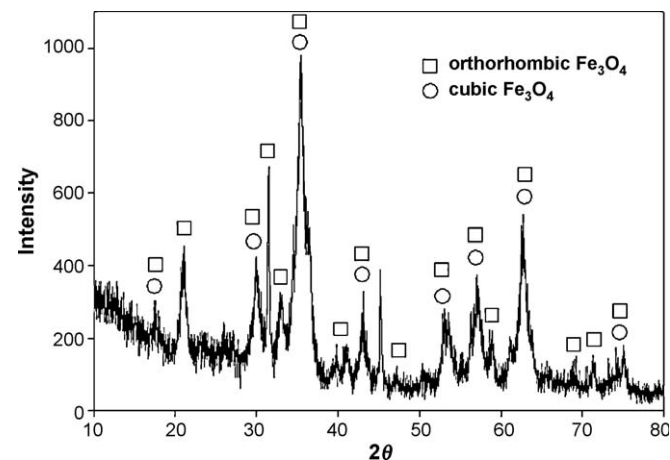


Fig. 2. XRD patterns of synthesized Fe_3O_4 . (Peaks of orthorhombic Fe_3O_4 (□); peaks of cubic Fe_3O_4 (○)).

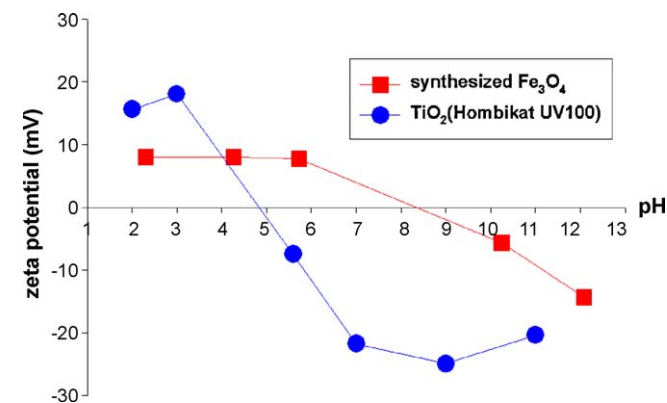


Fig. 3. Zeta potential differences between Fe_3O_4 and TiO_2 particles. (Fe_3O_4 (□); TiO_2 (○)).

dispersed solutions of two particles mix together at pH of 6. The particles color in the mixed solution changed to a pale yellow as shown in the picture of Fig. 4. TEM image of one sample particle shows that needle shape Fe_3O_4 particle was coated uniformly with TiO_2 particles to mask the reddish-brown color of Fe_3O_4 . XPS spectra in Fig. 5 show that the physical mixture of Fe_3O_4 and TiO_2 shows peaks of Fe_3O_4 , whereas peaks of Fe_3O_4 are barely visible in the XPS spectra of TiO_2 -masked Fe_3O_4 samples. The results conclude that the surface of Fe_3O_4 particle was well covered with TiO_2 particles in the TiO_2 -masked Fe_3O_4 particles.

Structure asymmetry and oxidation status of TiO_2 -masked Fe_3O_4 were investigated with XANES analysis. XANES analysis is the most informative technique for the determination of both local symmetry and oxidation state of transition metal ions [19–22]. All the Fe^{2+} and one half of the Fe^{3+} ions in Fe_3O_4 are located on 6-coordinate octahedral (O_h) sites while the other half of the Fe^{3+} ions are on 4-coordinate tetrahedral (T_d) sites. This asymmetry causes higher intensity of the $1s \rightarrow 3d$ transitions peaks in the pre-edge region [23,24]. The oxidation state of Fe ion can be related to the change in K-edge energy [23,24]. XANES spectra of various samples were shown in Fig. 6. Pre-edge energy and K-edge energies are summarized in Table 1. The intensities and positions of the $1s \rightarrow 3d$ pre-edge peaks between Fe_3O_4 and TiO_2 -masked Fe_3O_4 were similar (position: 7,114.2 eV, intensity: 0.13). This suggests that Fe_3O_4 and TiO_2 -masked Fe_3O_4 have similar asymmetric structures. However, the Fe K-edge energy of TiO_2 -masked Fe_3O_4 (7,127 eV) was higher than that of Fe_3O_4 (7,124.4 eV), but a little lower than that of Fe_2O_3 . This suggests that part of Fe^{2+} ions within Fe_3O_4 structure were changed to Fe^{3+} ions (with $\text{Fe}_3\text{O}_{4+\delta}$ formula) under close interaction with TiO_2 .

Fig. 7 shows catalytic activity for 1,2-dichlorobenzene (*o*-DCB) oxidation over various catalysts. Compared with Fe_3O_4 or TiO_2 particles that show 100% conversion at temperatures above 600 °C, TiO_2 -masked Fe_3O_4 exhibits much higher activity showing 100% conversion near 400 °C. There are two possibilities for the activity enhancement of TiO_2 -masked Fe_3O_4 : a synergistic effect due to physical contact between TiO_2 and Fe_3O_4 particles and formation of active sites on the $\text{Fe}_3\text{O}_{4+\delta}$ surface. To confirm first whether the activity enhancement results from the physical contact between TiO_2 and Fe_3O_4 particles, 3 different types of contact between Fe_3O_4 and TiO_2 particles were tested: (1) physical mixture of Fe_3O_4 and TiO_2 (weight ratio of $\text{Fe}_3\text{O}_4/\text{TiO}_2 = 1/19$); (2) a separate Fe_3O_4 bed at the top was in contact with a separate TiO_2 bed at the bottom; (3) top TiO_2 bed was in contact with bottom Fe_3O_4 bed (the reverse case of (2)). As shown in Fig. 7, there exists no activity

(a) The picture of TiO_2 -masked Fe_3O_4 (b) TEM images of TiO_2 -masked Fe_3O_4 **Fig. 4.** Images of TiO_2 -masked Fe_3O_4 . (a) Pictures of TiO_2 -masked Fe_3O_4 particles, (b) TEM image of TiO_2 -masked Fe_3O_4 .

enhancement for these three cases. It is therefore believed that the activity enhancement of TiO_2 -masked Fe_3O_4 is due to formation of active sites on the $\text{Fe}_3\text{O}_{4+\delta}$ species.

CO-TPR spectrum of the TiO_2 -masked Fe_3O_4 sample was compared with those of Fe_3O_4 and TiO_2 as shown in Fig. 8. Fe_3O_4 has a low intensity (arbitrary unit) and a broad peak around 300 °C. It is therefore believed that weakly adsorbed oxygen on the surface of Fe_3O_4 under air condition reacts with CO around 300 °C. Nano-sized particles contain abundant weakly adsorbed oxygen on the surface due to the large surface area [25]. TiO_2 has a moderate intensity with a peak around 420 °C. It has been known that CO begins to react with lattice oxygen above 400 °C, generating oxygen vacancies on the TiO_2 surface [26]. TiO_2 -masked Fe_3O_4 shows quite different TPR spectrum with three strong peaks. The first peak around 330 °C seems to be originated from the sites in Fe_3O_4 . Its intensity is increased slightly probably because oxygen adsorption is improved due to the electron deficient state of $\text{Fe}_3\text{O}_{4+\delta}$ species. The second peak around 420 °C is attributed to the peak from nano-sized TiO_2 in the TiO_2 -masked Fe_3O_4 . The third peak with strong intensity was observed around 460 °C. As discussed above, TiO_2 -masked Fe_3O_4 prepared by charge attraction between TiO_2 and Fe_3O_4 particles

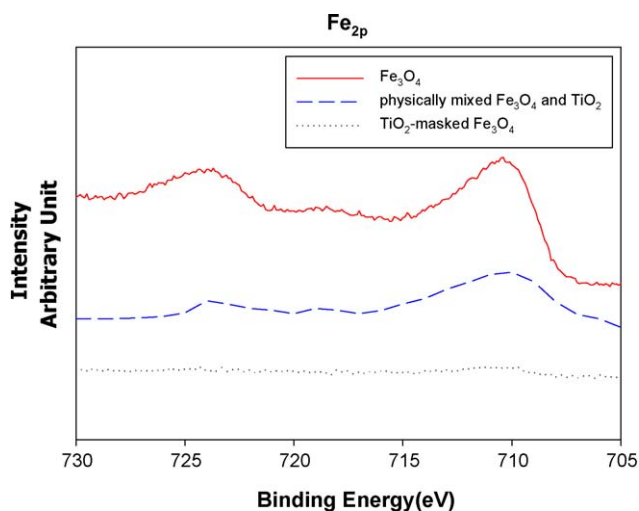
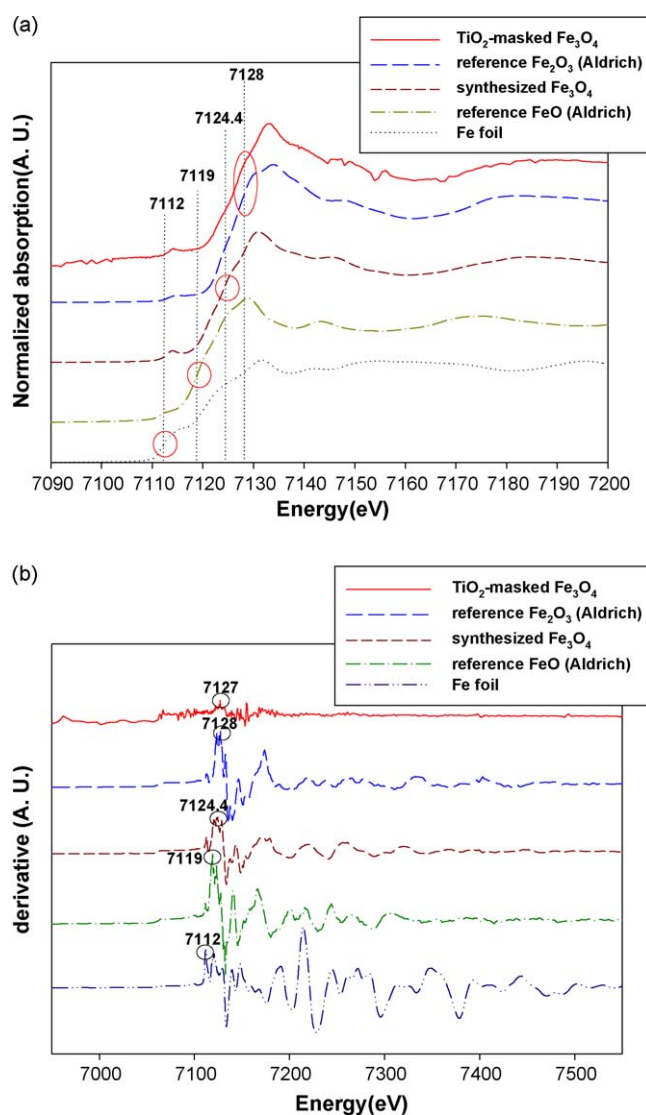
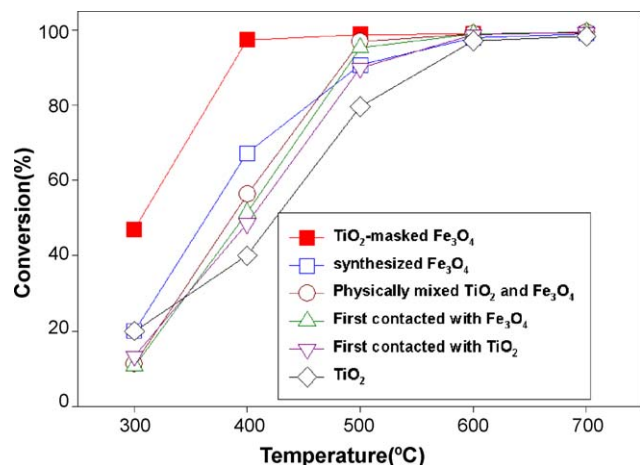
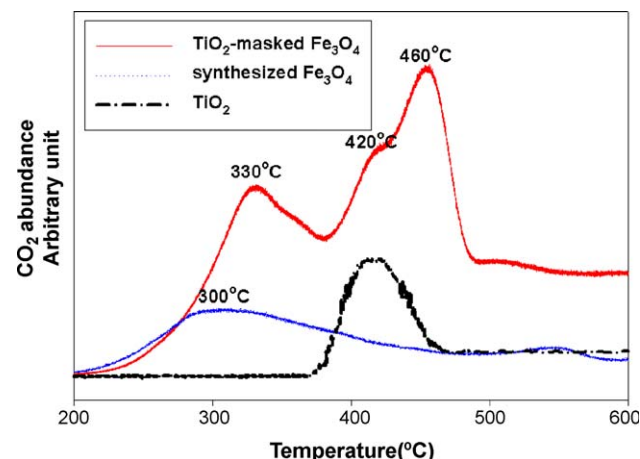
**Fig. 5.** XPS spectra of (a) Synthesized Fe_3O_4 , (b) Physically mixed Fe_3O_4 and TiO_2 , and (c) TiO_2 -masked Fe_3O_4 .**Fig. 6.** Fe K-edge XANES spectra of (a) TiO_2 -masked Fe_3O_4 , (b) reference Fe_2O_3 (Aldrich), (c) synthesized Fe_3O_4 , (d) reference FeO (Aldrich), and (e) pure Fe foil.

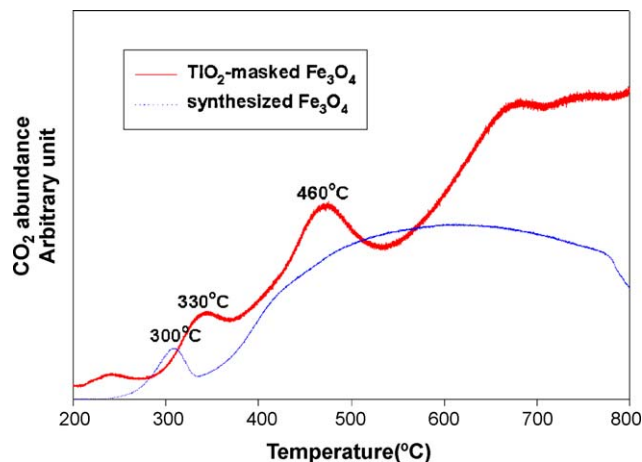
Table 1

Fe K-edge energy and the 1s → 3d pre-edge peak of the XANES spectra.

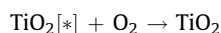
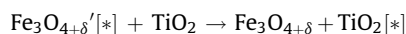
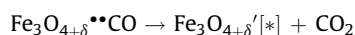
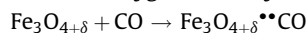
Sample	K-edge energy (eV)	Pre-edge peak	
		Position (eV)	Intensity
Fe metal	7112	–	–
FeO (reference)	7119	–	–
Synthesized Fe ₃ O ₄	7124.4	7114.1	0.13
Fe ₂ O ₃ (reference)	7128.4	7114.6	0.06
TiO ₂ -masked Fe ₃ O ₄	7127	7114.1	0.13

**Fig. 7.** Activity tests for o-DCB oxidation over TiO₂-masked Fe₃O₄ catalysts. (TiO₂-masked Fe₃O₄ (■); synthesized Fe₃O₄ (□); physically mixed Fe₃O₄ and TiO₂ (shaking for 1 h) (○); first contacted with Fe₃O₄ (□); first contacted with TiO₂ (▽); TiO₂ (◇)).**Fig. 8.** Temperature-programmed CO reduction. (TiO₂-masked Fe₃O₄ (solid line); synthesized Fe₃O₄ (dotted line); TiO₂ (dash-dot line)).

influences the oxidation state of Fe₃O₄, transforming some Fe²⁺ ions in the structure into Fe³⁺, which may provide strong CO adsorption sites to result in the appearance of the strong CO-TPR peak around 460 °C. Fe₃O_{4+δ} began to lose its excess oxygen by reacting with CO, and oxygen vacancies were consequently generated at temperatures above 460 °C. These oxygen vacancies could be strong adsorption sites for CO and other hydrocarbons. To further investigate the characteristics of reaction sites, CO-TPSR was carried out under a mixture stream of 1% CO/He and 3.5% O₂/He, as shown in Fig. 9. CO is normally

**Fig. 9.** Temperature-programmed surface reaction of CO with O₂. (TiO₂-masked Fe₃O₄ (solid line); synthesized Fe₃O₄ (dotted line)).

used as the probe molecule to identify the active sites [27]. For Fe₃O₄, a small TPSR peak around 300 °C was observed, which is similar to the results of CO-TPR. For TiO₂-masked Fe₃O₄, peak types of CO-TPSR are nearly the same as those of CO-TPR except that the second peak at 420 °C is not observed. The results indicate that CO adsorption sites in air (oxidizing environment) are originated from Fe₃O₄, not from TiO₂. The CO adsorption was enhanced by forming Fe₃O_{4+δ} in the TiO₂-masked Fe₃O₄. It is well known that oxygen species on TiO₂ became mobile at temperatures above 400 °C [25], thus mobile oxygen species that is transferred from TiO₂ can promote CO oxidation on the neighboring Fe₃O_{4+δ} sites. Liu et al. also reported that oxygen vacancy and mobility could be important properties for catalytic oxidation [28]. Therefore, a close contact between Fe₃O_{4+δ} and TiO₂ and the formation of Fe₃O_{4+δ} are responsible for the enhanced oxidation activity of the TiO₂-masked Fe₃O₄. The reaction mechanism can be expressed as follows, where [*] refers to oxygen vacancy in Fe₃O_{4+δ} and TiO₂.



Even though TiO₂-masked Fe₃O₄ exhibits much higher activity for CO oxidation, Fe₃O₄ itself also shows relatively good catalytic activity for CO oxidation with a broad peak at temperatures above 400 °C due to formation of Fe₂O₃ phase. CO oxidation on Fe₂O₃ with and without O₂ has been reported in many papers [29,30]. For the high temperature incineration, however, the thermal stability of catalyst is also another important factor, and we believe that TiO₂-coated Fe₃O₄ would be much more stable than nano particles of iron oxides. Moreover, when embedded inside polymer, TiO₂-masked Fe₃O₄ particles are more color-masked (colorless) for easy coloring of the polymer products.

3.2. Catalyst-embedded polymers

Catalysts-embedded PE and PS were prepared with three different catalysts of Fe₃O₄, TiO₂ and TiO₂-masked Fe₃O₄. Compared with Fe₃O₄-embedded polymers, the color degree in polymer composites embedded with TiO₂-masked Fe₃O₄ particles are greatly weakened because the outside layer of TiO₂ particles

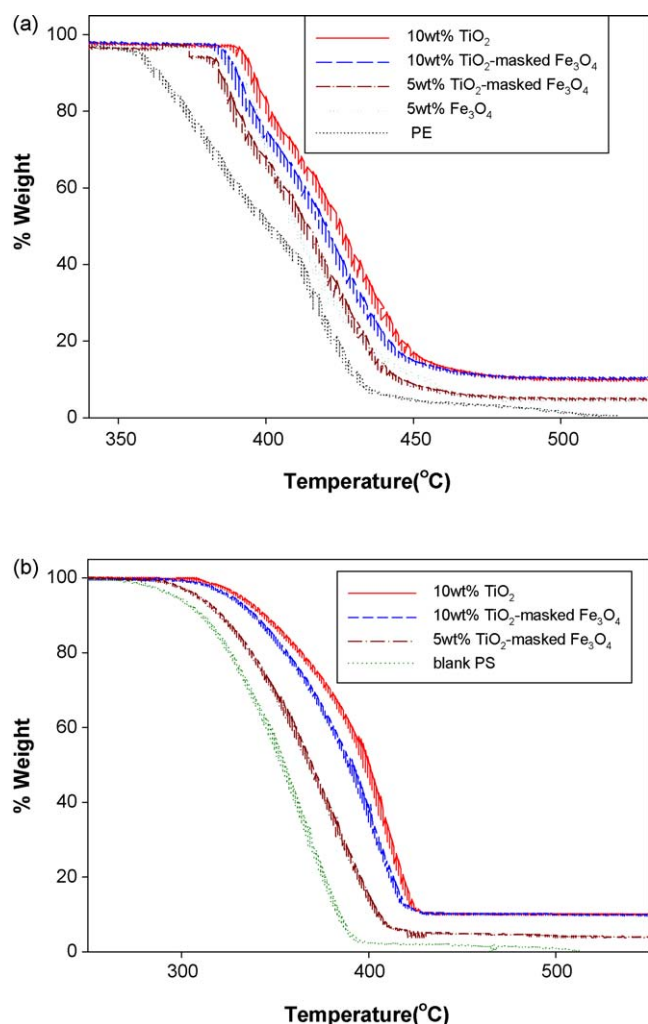


Fig. 10. TGA results of (a) poly ethylene (PE) and (b) poly styrene (PS) containing various catalysts.

effectively mask the red-brown color of Fe_3O_4 . The decomposition temperatures of PE and PS composites increased with catalyst content as shown in TGA spectra of Fig. 10. As the additive is added inside polymer, the thermal stability of catalysts/polymer composites can be improved due to the restriction of mobility of polymer chains, trapping effects and a change in thermal conductivity [31–34]. These improvements in thermal stability are important for the polymer blending. Therefore, TiO_2 -masked Fe_3O_4 would be a good candidate as polymer additives for preventing degradation at fabrication stage.

In order to check the oxidation activity of embedded catalysts, incineration tests were carried out. During the incineration of polymers, hydrocarbons of low molecular weight would be generated as volatile compounds or adsorbed on potential active sites. Additives could act as oxidation catalysts for low molecular hydrocarbons. Fig. 11 and Tables 2 and 3 show quantitative analysis of CO_2 emission during incineration of various PE and PS composite chips. It was confirmed that CO_2 emissions were affected by the type and amount of embedded catalyst. PE and PS that were embedded with TiO_2 -masked Fe_3O_4 particles had better activity for direct oxidation into CO_2 than PE and PS that contain pure TiO_2 or Fe_3O_4 particles. At present, we did not measure other carbon sources such as hydrocarbons, CO or carbon residue. Later we should need more research about the rest of carbon sources in detail.

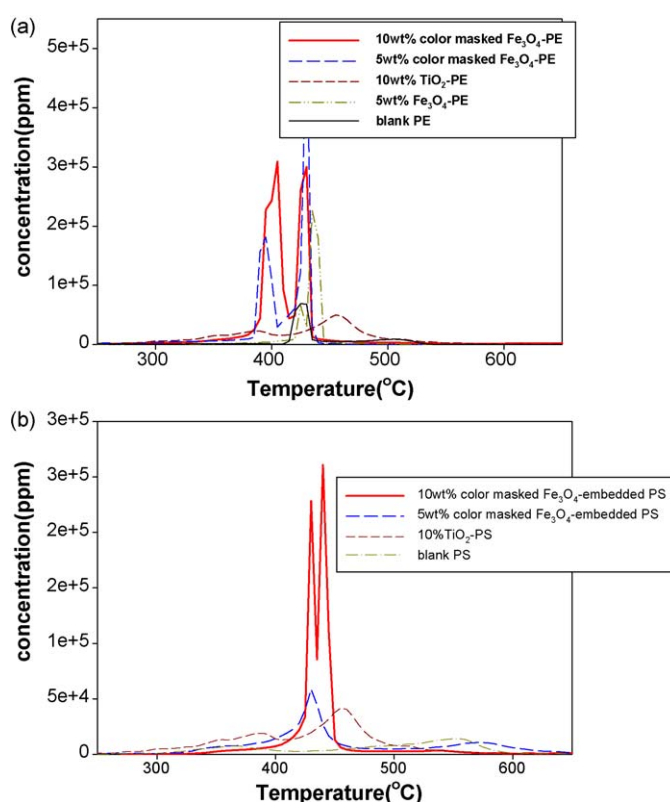


Fig. 11. Quantitative analysis of CO_2 emission during the incineration of (a) PE and (b) PS samples.

Table 2

CO_2 emission during incineration of poly ethylene.

Polymer	Area of CO_2 profile (ppm K)	CO_2 wt.% (g of carbon in CO_2 /g of carbon in polymer)
PE	1.854×10^6	12%
5 wt.% Fe_3O_4 in PE	3.049×10^6	19.7%
10 wt.% TiO_2 in PE	4.608×10^6	29.8%
5 wt.% TiO_2 -masked Fe_3O_4 in PE	7.392×10^6	47.8%
10 wt.% TiO_2 -masked Fe_3O_4 in PE	9.584×10^6	62%

Table 3

CO_2 emission during incineration of poly styrene.

Polymer	Area of CO_2 profile (ppm K)	CO_2 wt.% (g of carbon in CO_2 /g of carbon in polymer)
PS	1.867×10^6	11%
10 wt.% TiO_2 in PS	3.840×10^6	22.6%
5 wt.% TiO_2 -masked Fe_3O_4 in PS	3.269×10^6	19.3%
10 wt.% TiO_2 -masked Fe_3O_4 in PS	9.663×10^6	56.9%

4. Conclusions

Nano-sized Fe_3O_4 particle that was covered with a porous layer of nano-sized TiO_2 particles was prepared by simply controlling pH of aqueous slurry solution of the two particles, utilizing different values of isoelectric point (IEP coating method). We could confirm an effective covering of Fe_3O_4 particle with TiO_2 particles from XPS and TEM results, and a color-masking effect of red-brown color into a pale yellow. XANES analyses confirm that parts of the Fe^{2+} ions were changed to Fe^{3+} ions within the Fe_3O_4 structure (with $\text{Fe}_3\text{O}_{4+\delta}$ formula) due to a close interaction of Fe_3O_4 particle with

TiO₂ particles during the IEP coating. Fe₃O_{4+δ} species is believed to have potential catalytic sites for the oxidation of o-DCB and CO. More specifically, we can guess that active sites on Fe₃O_{4+δ} play roles for the adsorption and reaction and TiO₂ plays a role for providing oxygen molecule to Fe₃O_{4+δ} sites from CO-TPR and CO-TPSR analyses.

TiO₂-masked Fe₃O₄ particles that were embedded in polymers showed a good color-masking effect and could improve the thermal stability of base polymers during high temperature fabrication. Polyethylene and polystyrene that were embedded with TiO₂-masked Fe₃O₄ particles enhanced the generation of CO₂ during the incineration, indicating to us that catalyst-embedded polymers can reduce noxious emissions, including volatile hydrocarbons, during the thermal incineration of polymers.

Acknowledgements

The authors gratefully acknowledge the support from the Brain Korea 21 project, the Korea Institute of Science and Technology Evaluation and Planning (KISTEP, M1-0214-00-0133), and the Korea Science and Engineering Foundation (KOSEF, M02-2004-000-10512-0).

References

- [1] D.J. Paustenbach, *Regul. Toxicol. Pharmacol.* 36 (2002) 211–219.
- [2] K. Olie, P.L. Vermeulen, O. Hutzinger, *Chemosphere* 6 (1977) 455–459.
- [3] R. Weber, M. Plinke, Z. Xu, M. Wilken, *Appl. Catal. B* 31 (2001) 195–207.
- [4] H. Mätzing, W. Baumann, B. Becker, K. Jay, H.R. Paur, H. Seifert, *Chemosphere* 42 (2001) 803–809.
- [5] S. Nagano, H. Tamon, T. Adzumi, K. Nakagawa, T. Suzuki, *Carbon* 38 (2000) 915–920.
- [6] M. Hiraoka, N. Takeda, S. Okajima, T. Kasakura, Y. Imoto, *Chemosphere* 19 (1989) 361–366.
- [7] M. Okumura, T. Akita, M. Haruta, X. Wang, O. Kajikawa, O. Okada, *Appl. Catal. B* 41 (2003) 43–52.
- [8] S.D. Yim, D.J. Koh, I.S. Nam, *Catal. Today* 75 (2002) 269–276.
- [9] R. Weber, T. Sakurai, H. Hagenmaier, *Appl. Catal. B* 20 (1999) 249–256.
- [10] P.L. Beltrame, P. Carniti, G. Audisio, F. Bertini, *Polym. Degrad. Stab.* 26 (1989) 209–220.
- [11] R.C. Mordí, R. Fields, J. Dwyer, *J. Anal. Appl. Pyrolysis* 29 (1994) 45–55.
- [12] Y. Uemichi, Y. Makino, T. Kanazuka, *J. Anal. Appl. Pyrolysis* 14 (1989) 331–344.
- [13] T. Imai, T. Matsui, Y. Fujii, T. Nakai, S. Tanaka, *J. Mater. Cycles Waste Manag.* 3 (2001) 103–109.
- [14] Y.S. Kang, S. Risbud, J.F. Rabolt, P. Stroeve, *Chem. Mater.* 8 (1996) 2209–2211.
- [15] S. Krishnamoorthy, J.P. Baker, M.D. Amiridis, *Catal. Today* 40 (1998) 39–46.
- [16] G.G. Dvoryankina, Z.G. Pinsker, *J. Appl. Phys.* 132 (1960) 110–113.
- [17] M. Iizumi, T.F. Koetzle, G. Shirane, S. Chikazumi, M. Matsui, S. Todo, *Acta Crystallogr. B* 38 (1982) 2121–2133.
- [18] G.K. Williamson, W.H. Hall, *Acta Metall.* 1 (1953) 22–31.
- [19] C. Lamberti, S. Bordiga, F. Bonino, C. Prestipino, G. Berlier, L. Capello, F. D'Acapito, F.X. Llabrés i Xamena, A. Zecchina, *Phys. Chem. Chem. Phys.* 5 (2003) 4502–4509.
- [20] C. Lamberti, C. Prestipino, S. Bordiga, G. Berlier, G. Spoto, A. Zecchina, A. Laloni, F. La Manna, F. Danca, R. Felici, F. D'Acapito, P. Roy, *Nucl. Instrum. Methods Phys. Res. B* 200 (2003) 196–201.
- [21] C. Lamberti, G. Turnes Palomino, S. Bordiga, G. Berlier, F. D'Acapito, A. Zecchina, *Angew. Chem. Int. Ed.* 39 (2000) 2138–2141.
- [22] C. Lamberti, C. Prestipino, F. Bonino, L. Capello, S. Bordiga, G. Spoto, A. Zecchina, S. Diaz Moreno, B. Cremaschi, M. Garilli, A. Marsella, D. Carmello, S. Vidotto, G. Leofanti, *Angew. Chem. Int. Ed.* 41 (2002) 2341–2344.
- [23] L.W. Lin, Y. Kou, M. Zou, Z. Yan, *Phys. Chem. Chem. Phys.* 3 (2001) 1789–1794.
- [24] G. Berlier, M. Pourny, S. Bordiga, G. Spoto, A. Zecchina, C. Lamberti, *J. Catal.* 229 (2005) 45–54.
- [25] H. Berndt, I. Pitsch, S. Evert, K. Struve, M.-M. Pohl, J. Radnik, A. Martin, *Appl. Catal. A* 244 (2003) 169–179.
- [26] H. Kim, D.W. Park, H.C. Woo, J.S. Chung, *Appl. Catal. B* 19 (1998) 233–243.
- [27] Y.J. Huang, J.A. Schwarz, *Appl. Catal.* 30 (1987) 239–253.
- [28] W. Liu, A.F. Sarofim, M. Flytzani-Stephanopoulos, *Appl. Catal. B* 4 (1994) 167–186.
- [29] P. Li, D.E. Miser, S. Rabiei, R.T. Yadav, M.R. Hajaligol, *Appl. Catal. B* 43 (2003) 151–162.
- [30] J.-L. Cao, Y. Wang, X.-L. Yu, S.-R. Wang, S.-H. Wu, Z.-Y. Yuan, *Appl. Catal. B* 79 (2008) 26–34.
- [31] G. Qiu, Q. Wang, C. Wang, W. Lau, Y. Guo, *Ultrason. Sonochem.* 14 (2007) 55–61.
- [32] Y. Feng, L.N. Gordon, *J. Appl. Polym. Sci.* 91 (2004) 3844–3850.
- [33] Y.H. Hu, C.Y. Chen, C.C. Wang, *Polym. Degrad. Stab.* 84 (2004) 545–553.
- [34] T.C. Chang, Y.T. Wang, Y.S. Hong, Y.S. Chiu, *J. Polym. Sci. A Polym. Chem.* 38 (2000) 1972–1980.